JACS
JOURNAL OF THE AMERICAN CHEMICAL SOCIETY

Communication

pubs.acs.org/JACS

Dual-Emitting Quantum Dot/Quantum Rod-Based Nanothermometers with Enhanced Response and Sensitivity in Live Cells

Aaron E. Albers, Emory M. Chan, Patrick M. McBride, Caroline M. Ajo-Franklin, Bruce E. Cohen,* and Brett A. Helms*

The Molecular Foundry, Lawrence Berkeley National Laboratory, Berkeley, California 94720, United States

Supporting Information

ABSTRACT: Temperature is a key parameter in physiological processes, and probes able to detect small changes in local temperature are necessary for accurate and quantitative physical descriptions of cellular events. Several have recently emerged that offer excellent temperature sensitivity, spatial resolution, or cellular compatibility, but it has been challenging to realize all of these properties in a single construct. Here, we introduce a luminescent nanocrystal-based sensor that achieves this with a 2.4% change/°C ratiometric response over physiological temperatures in aqueous buffers, with a precision of at least 0.2 °C. Thermoresponsive dual emission is conferred by a Förster resonant energy transfer (FRET) process between CdSe−CdS quantum dot−quantum rods (QD−QRs) as donors and cyanine dyes as acceptors, which are conjugated to QD−QRs using an amphiphilic polymer coating. The nanothermometers were delivered to live cells using a pH-responsive cationic polymer colloid, which served to both improve uptake and release nanocrystals from endosomal confinement. Within cells, they showed an unexpected enhancement in their temperature response and sensitivity, highlighting the need to calibrate these and similar probes within the cell.

Temperature pervades our description of even the most basic of physical, chemical, and biological phenomena. Carrying out thermometry with greater precision,[1] under difficult experimental circumstances,[2] in a nonperturbative manner[3] or at extreme length scales[4] continues to drive innovation in both materials and instrumentation. A particularly compelling system to investigate that encompasses the breadth of these difficulties is the interior of a live cell. Here, exceptionally precise measurements may be required to discern subtle temperature inhomogeneities within the cell and to relate their dynamics. Small variations—even in seemingly homothermic cells—are likely to affect cellular events, including diffusion, protein folding, or enzyme catalysis. Quantification of local temperature transients in the cytosol nevertheless remains elusive.

Luminescent temperature-sensitive materials offer a promising avenue for thermometry in live cells in that their intensity or decay lifetime can relate temperature if properly calibrated. Temperature-dependent luminescent probes based on organic dyes and polymers, while synthetically accessible, generally display poor photostability and pronounced cross-sensitivity to oxygen, which is undesirable for live cell work.[5] Thermometric fluorescent proteins[6] have also been investigated and are biocompatible; however, there is a strong pH dependence on the lifetime of the fluorophore, which makes it difficult to use without simultaneously measuring the pH of the environment being surveyed. Nanothermometers based on both pure and doped semiconductor nanocrystals have been recently reported.[7] Impressive temperature sensitivity in buffer was demonstrated, although their cytosolic compatibility remains untested. Luminescent nanophosphors have likewise been deployed as vesicle-bound temperature probes in cells, although their sensitivity is limited in the normal physiological range.[8] The outstanding challenge faced by luminescent thermometers is concomitant realization of brightness, photostability, sensitivity, and precision at T = 20−40 °C when probing subcellular microenvironments.

We show here that hybrid nanomaterials based on polymer-wrapped CdSe−CdS quantum dot−quantum rod (QD−QRs) functionalized with temperature-responsive cyanine dyes address these issues in a single construct and exhibit enhanced thermometric response and sensitivity when translocated to the cytosol. By modeling optical changes in the nanocrystals components as a function of temperature, we find that response of this construct is also well explained by the change in quantum yield of the CdSe−CdS QD−QRs versus the cyanine dye and the red shift in QD−QR emission with increasing temperature.

The molecular design of dual-emitting ratiometric nanothermometers (NanoTs) features a red-emitting CdSe−CdS QD−QR semiconductor nanocrystal heterostructure passivated with an amphiphilic polymer shell, to which is appended far-red emitting cyanine dyes (Scheme 1). QD−QRs have giant extinction coefficients[9] owing to their CdS shells, and bright temperature-responsive luminescence due to well-behaved shifts in their bandgap (Figure S2). Cyanine dyes[10] (e.g., Alexa Fluor 647), on the other hand, show temperature-dependent fluorescence quantum yields but no wavelength shifts (Figure S3). Together, they constitute FRET pairs with thermoresponsive character ideal for ratiometric imaging: their internally calibrated, strong optical read-out should translate to

Received: March 19, 2012
Published: May 29, 2012

dx.doi.org/10.1021/ja302290e | J. Am. Chem. Soc. 2012, 134, 9565−9568

Scheme 1. Chemical Synthesis of Dual-Emitting Hybrid Nanothermometers

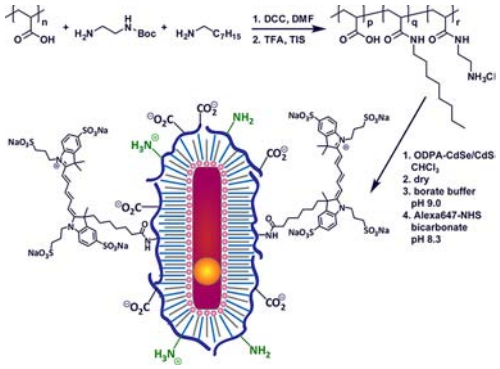

more reliable and precise temperature measurements in cells than is possible otherwise using conventional FRET donors like quantum dots, which are at least an order of magnitude less bright than QD−QRs.[9b]

We synthesized red-emitting CdSe−CdS QD−QRs using an automated nanocrystal synthesis robot[11] (Symyx Technologies), with 4-nm diameter CdSe cores used to seed the epitaxial growth of CdS rods (see Supporting Information). The absorption peak of the first exciton was observed at 613 nm, with an emission maximum at 617 nm and a photoluminescence quantum yield (Φ_{QD-QR}) of 0.74. TEM revealed an aspect ratio of ∼5:1 (Figure S1). QD−QRs were transferred into water using a poly(acrylic acid)-based amphiphilic random copolymer displaying an optimized ratio of hydrophobic alkyl chains, carboxylic acids, and alkylamines (Scheme 1). Polymer-wrapped QD−QRs (Φ_{QD-QR} = 0.70) were ∼20 nm in average hydrodynamic diameter after purification by size exclusion chromatography (Figure S2).

QD−QRs were labeled with temperature-responsive Alexa-647 dyes, ∼9−12 per QD−QR depending on the batch, to give the final hybrid nanothermometer construct (diameter = 23 nm, Figure S2). Upon labeling, the emission of the QD−QRs in the NanoTs was substantially reduced due to FRET (Figure S5), with energy transfer efficiencies (E_m) range of 75−90%, depending on the number of dyes (m) per QD−QR. For NanoTs with m = 9 and E_m = 89%, we calculated the Förster radius (R_o) as 7.3 nm. The average separation between the donor and acceptors was determined to be ∼7.5 nm (see Supporting Information). This separation is consistent with the native ligand shell persisting in the final material, the additional 3−4 nm afforded by the polymer wrapping, and the aliphatic linker from the Alexa-647 dye to the polymer. We also noted that the emission intensity of the Alexa-647 dye was ∼20% from what would be expected with 89% energy transfer from the QD−QR and the quantum yield of unbound Alexa-647 in solution (Φ_{A647} = 0.33); this decrease likely arises from an increase in the nonradiative decay for Alexa-647 when tethered to the QD−QR.

Both QD−QRs and Alexa-647 dyes show temperature dependent emission upon direct excitation (Figure S3). In the case of QD−QRs, the temperature-dependent shift of the emission maximum to longer wavelengths ($\Delta\lambda_{em}$ = 2 nm for T = 20−40 °C) is accompanied by modest decrease in Φ_{QD-QR} (Φ_{QD-QR} = 0.65 at T = 40 °C). These changes are fully reversible in aqueous buffer over the temperature range examined, indicating that the polymer-wrapped QD−QRs do not undergo any photodecomposition in the process and suggesting that the temperature dependence of the optical properties can be therefore ascribed to changes in the band gap with increasing temperature. Similar behavior as described by the Varshni equation has been observed in related core−shell heterostructures.[12] For Alexa-647, the emission substantially decreases from T = 20−40 °C (Φ_{A647} = 0.20 at T = 40 °C). The extended polyene bridge between the indolium groups is susceptible to molecular rotation. At higher temperatures, the greater frequency of this 'wagging' of the polyene bridge decreases the fluorescence quantum yield but does not shift the emission maximum[10c,d] (Figure S3).

FRET-enabled hybrid NanoTs exhibited a highly sensitive temperature response in the physiological range (T = 20−40 °C) upon excitation at λ_{ex} = 400 nm (Figure 1A). As was the case for the individual luminescent species, a slight shift in emission wavelength from the QD−QR was observed, as was a decrease in intensity; for the Alexa-647, only a decrease in the emission intensity was evident. To calibrate the temperature-responsive dual emission of the NanoTs, we selected the region near the band edge of the QD−QR ($I_{630-640}$) where the integrated intensity undergoes a small change along with the region where Alexa-647 is most temperature responsive ($I_{664-674}$). The calculated and observed ratiometric responses, $R = I_{630-640}/I_{664-674}$, for T = 20−40 °C in 5 °C increments is shown in Figure 1B for 3 cycles of heating and cooling, where each measurement is taken 3 times at a given temperature following a 10 min equilibration period. The data indicate that

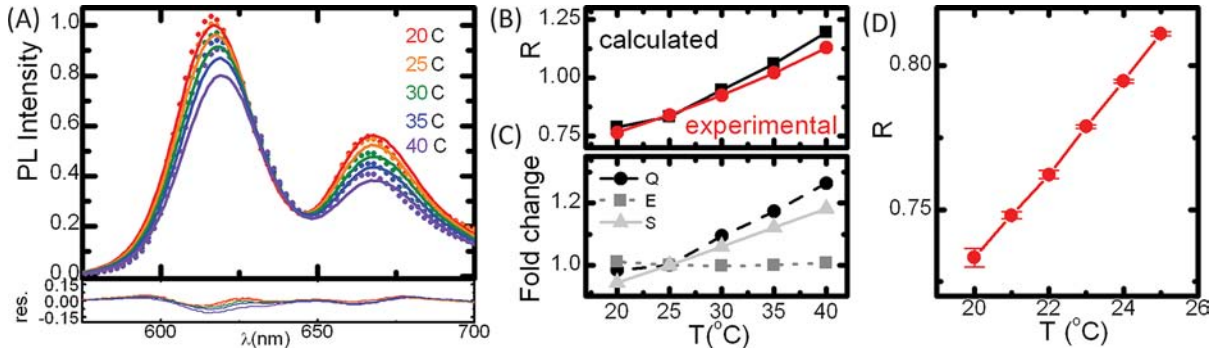

Figure 1. NanoTs show sensitive, reproducible spectral changes in response to temperature: (A) calculated (dots) and observed (solid lines) temperature-dependent emission from NanoTs with ∼12 Alexa-647 dyes conjugated to their periphery; (B) ratiometric response, $R = I_{630-640}/I_{664-674}$; (C) the fold change in Alexa-647 fluorescence quantum yield (Q, circles), FRET efficiency (E, squares), and QD−QR emission shift (S, triangles) relative to T = 25 °C (see Supporting Information); (D) ratiometric response of NanoTs for T = 20−25 °C.

dx.doi.org/10.1021/ja302290e | J. Am. Chem. Soc. 2012, 134, 9565−9568

hysteresis is negligible and that the constructs are photostable for the duration of the 5 h experiment. Over a more focused temperature range of T = 20−25 °C in 1 °C increments (Figure 1D), the pseudolinear ratiometric response showcased the sensitivity of the NanoTs at ∼2.4%/°C. The precision with which these optical measurements relate temperature was at least 0.2 °C (Figure S6), a value limited by the precision of the Peltier temperature controller used in these experiments and comparable to other nanocrystal-based optical thermometers.[7b] This capability is essential given recent work showing subcellular inhomogeneities of or below 1 °C, for example, near mitochondria.[5a]

We modeled the NanoT temperature response from T = 20−40 °C as a weighted sum of the QD−QR and Alexa-647 emission spectra at that same temperature (see Supporting Information). Experimentally determined inputs into this model included the temperature dependent QD−QR and Alexa-647 emission spectra (Figure S3) and three parameters from the NanoT emission spectrum at T = 25 °C, derived from the peak positions of the QD−QR and Alexa-647 emission and the apparent Alexa-647 quantum yield in the NanoTs. As shown in Figure 1A, this approach yielded good agreement between the predicted and observed spectra. Moreover, the values of the ratiometric response R calculated from the predicted spectra recapitulate the temperature dependence observed for the NanoTs (Figure 1B). The temperature-dependence of R reflects contributions from Φ_{QD-QR}/Φ_{A647} (Q), the degree of energy transfer (E), and the QD−QR emission red-shift (S) (see Supporting Information). This analysis shows that the increase in R with temperature reflects nearly similar contributions from the dramatic decrease in Φ_{A647} relative to Φ_{QD-QR} and from the gradual red-shift of the QD−QR emission, and that the calculated energy transfer efficiency is essentially constant (Figure 1C).

Given the sensitivity, precision, and well-behaved optical response of the NanoTs over 20−40 °C in aqueous buffers, we introduced them into cells as local optical thermometers. We recently reported a strategy to translocate nanocrystals to the cytosol using pH-responsive cationic polymer colloids,[13] to which the probes are conveniently adsorbed via complementary electrostatic interactions. With these unusual materials, it is possible to leverage the low pH of late endosomes to increase the volume of the colloid ∼30-fold, which disrupts the confining membrane and leads to cytosolic delivery of the nanocrystals. To determine whether these colloids could mediate NanoT delivery into live cells, we incubated either human epithelial cells or mouse fibroblasts with NanoTs adsorbed onto the colloids and quantified the labeling efficiency using flow cytometry (Figure 2). With HeLa cells, unmediated delivery of NanoTs did not proceed efficiently as evidenced by the insignificant signal above background compared to untreated cells. In contrast, vector-mediated delivery by the cationic polymer colloid afforded a geometric mean photoluminescence intensity (PL) ∼20-fold above background. Similar enhancement in the delivery using the cationic polymer colloids was observed with NIH 3T3 cells. This endothelial cell line recycles membrane constituents more rapidly than HeLa cells; thus, in the unmediated delivery, some signal above background could be observed (2.8-fold). Nevertheless, a dramatic increase in the labeling efficiency (>200-fold) was recorded for the vector-mediated process, pointing to the unique opportunity of these pH-responsive polymer colloids to enable cytosolic, live cell thermometry with our NanoTs.

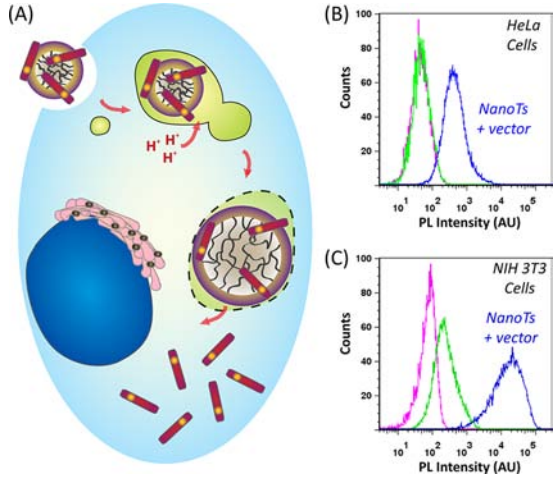

Figure 2. Flow cytometry enables quantitative comparison of nanothermometer delivery efficacy (A) to either HeLa or NIH 3T3 cells (B or C, respectively): cells incubated without NanoTs (pink), 5 nM NanoTs (green), or 5 nM NanoTs in the presence of 3 μg mL^{-1} of endosome-disrupting polymer colloid (blue).

Having determined a method for their introduction into cells, we next sought to determine how the NanoTs behaved within the cytosol. The optical response of the NanoTs inside HeLa cells was recorded at both T = 20 and 25 °C, and the ratiometric response calculated as before and compared to the response in buffer (Figure 3). We noted that both the absolute

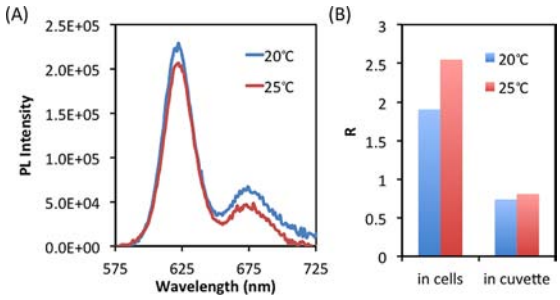

Figure 3. Photoluminescence (A) and ratiometric responses (B) from NanoTs in the cytosol of live HeLa cells or in 100 mM bicarbonate buffer pH 8.3 at T = 20 °C (blue) or 25 °C (red).

value of the ratiometric response and the magnitude of its modulation at higher temperature were enhanced compared to experiments taken in aqueous buffers. This unexpected phenomenon in optical response inside cells may involve a specific response of the dyes to cytosolic constituents.[10c−e] Given the extent of QD−QR quenching by appended Alexa-647 dyes is lower in cells than in buffers suggests several possible explanations: either the cyanine dye is degrading in the cell, or its average distance to the QD−QR increases once in the cytosol. The former can be rationalized by the presence of endogenous thiols in the cytosol, which have been shown to photoreversibly react with the polyene bridge,[10c] while the later may be due to a protein corona[14] forming at the surface of the NanoT. With respect to the enhanced intracellular temperature sensitivity of the Alexa-647 emission, cytosolic viscosity may be responsible, in particular because neither Alexa-647 or polymer-wrapped QD−QRs exhibit solvatochromism.[15] The dramatic differences between cellular and cuvette measurements highlight the importance of calibrating probes within a cell, rather

dx.doi.org/10.1021/ja302290e | J. Am. Chem. Soc. 2012, 134, 9565−9568

than using buffer as a proxy for the cytosol. Future work in establishing these metrics for different cell types is a critical next step for using NanoTs in cell-based assays.

We have described here the synthesis, characterization, and modeling of dual-emitting ratiometric optical nanothermometers, whose response and sensitivity is unexpectedly enhanced when delivered to the cytosol of live cells. As such, the results presented here seed new avenues of research in the biophysical and biomedical sciences; sensitive optical nanocrystal-based probes that are able to detect subtle changes in temperature in the cytosol of live cells are ideally suited for fundamental explorations into subcellular thermometry and thermogenesis. They should also find use in quantitative high-throughput optical screens of new drug candidates for treating metabolic disorders such as obesity.

■ ASSOCIATED CONTENT

Supporting Information

Detailed experimental procedures regarding the synthesis, characterization, modeling, and biological protocols for all materials. This material is available free of charge via the Internet at http://pubs.acs.org.

■ AUTHOR INFORMATION

Corresponding Author

becohen@lbl.gov; bahelms@lbl.gov

Notes

The authors declare no competing financial interest.

■ ACKNOWLEDGMENTS

We thank Cheryl Goldbeck for assistance with flow cytometry and Teresa E. Pick and Dev S. Chahal for extensive initial exploratory syntheses and TEM. All work was performed at the Molecular Foundry and was supported by the Director, Office of Science, Office of Basic Energy Sciences, Division of Materials Sciences and Engineering, of the U.S. Department of Energy under Contract No. DE-AC02-05CH11231.

■ REFERENCES

(1) Marcus, G. A.; Schwettman, H. A. *J. Phys. Chem. B* **2007**, *111*, 3048−3054.

(2) (a) Rigolini, J.; Bombled, F.; Ehrenfeld, F.; El Omari, K.; Le Guer, Y.; Grassl, B. *Macromolecules* **2011**, *44*, 4462−4469. (b) Pekala, K.; Wisniewski, A.; Jurczakowski, R.; Wisniewski, T.; Wojdyga, M.; Orlik, M. *J. Phys. Chem. A* **2010**, *114*, 7903−7911.

(3) (a) Koptyug, I. V.; Khomichev, A. V.; Lysova, A. A.; Sagdeev, R. Z. *J. Am. Chem. Soc.* **2008**, *130*, 10452−10453. (b) Doerk, G. S.; Carraro, C.; Maboudian, R. *ACS Nano* **2010**, *4*, 4908−4914.

(4) (a) Sadat, S.; Tan, A.; Chua, Y. J.; Reddy, P. *Nano Lett.* **2010**, *10*, 2613−2617. (b) Hoffmann, E. A.; Nilsson, H. A.; Matthews, J. E.; Nakpathomkun, N.; Persson, A. I.; Samuelson, L.; Linke, H. *Nano Lett.* **2009**, *9*, 779−783.

(5) (a) Okabe, K.; Inada, N.; Gota, C.; Harada, Y.; Funatsu, T.; Uchiyama, S. *Nat. Commun.* **2012**, *3*, No. 705. (b) Ye, F.; Wu, C.; Jin, Y.; Chan, Y.-H.; Zhang, X.; Chiu, D. T. *J. Am. Chem. Soc.* **2011**, *133*, 8146−8149. (c) Gota, C.; Okabe, K.; Funatsu, T.; Harada, Y.; Uchiyama, S. *J. Am. Chem. Soc.* **2009**, *131*, 2766−2767. (d) Gota, C.; Uchiyama, S.; Yoshihara, T.; Tobita, S.; Ohwada, T. *J. Phys. Chem. B* **2008**, *112*, 2829−2836. (e) Barilero, T.; Le Saux, T.; Gosse, C.; Jullien, L. *Anal. Chem.* **2009**, *81*, 7988−8000. (f) Shiraishi, Y.; Miyamoto, R.; Hirai, T. *Langmuir* **2008**, *24*, 4273−4279. (g) Uchiyama, S.; de Silva, A. P.; Iwai, K. *J. Chem. Educ.* **2006**, *83*, 720. (h) Lou, J.; Hatton, T. A.; Laibinis, P. E. *Anal. Chem.* **1997**, *69*, 1262−1264. (i) Fister, J. C.; Rank, D.; Harris, J. M. *Anal. Chem.* **1995**, *67*, 4269−4275. (j) Schrum, K. F.; Williams, A. M.; Haerther, S. A.; Ben-Amotz, D. *Anal. Chem.* **1994**, *66*, 2788−2790. (k) Kubin, R. F.; Fletcher, A. N. *J. Lumin.* **1982**, *27*, 455−462.

(6) (a) Wong, F. H. C.; Banks, D. S.; Abu-Arish, A.; Fradin, C. *J. Am. Chem. Soc.* **2007**, *129*, 10302−10303. (b) Leiderman, P.; Huppert, D.; Agmon, N. *Biophys. J.* **2006**, *90*, 1009−1018.

(7) (a) Hsia, C.-H.; Wuttig, A.; Yang, H. *ACS Nano* **2011**, *5*, 9511−9522. (b) McLaurin, E. J.; Vlaskin, V. A.; Gamelin, D. R. *J. Am. Chem. Soc.* **2011**, *133*, 14978−14980. (c) Maestro, L. M.; Jacinto, C.; Silva, U. R.; Vetrone, F.; Capobianco, J. A.; Jaque, D.; Sole, J. G. *Small* **2011**, *7*, 1774−1778. (d) Yang, J.-M.; Yang, H.; Lin, L. *ACS Nano* **2011**, *5*, 5067−5071. (e) Maestro, L. M.; Rodríguez, E. M.; Rodríguez, F. S.; Iglesias-de la Cruz, M. C.; Juarranz, A.; Naccache, R.; Vetrone, F.; Jaque, D.; Capobianco, J. A.; Sol, J. G. *Nano Lett.* **2010**, *10*, 5109−5115. (f) Vlaskin, V. A.; Janssen, N.; van Rijssel, J.; Beaulac, R.; Gamelin, D. R. *Nano Lett.* **2010**, *10*, 3670−3674. (g) Chin, P. T. K.; de Mello Donegá, C.; van Bavel, S. S.; Meskers, S. C. J.; Sommerdijk, N. A. J. M.; Janssen, R. A. J. *J. Am. Chem. Soc.* **2007**, *129*, 14880−14886. (h) Lee, J.; Govorov, A. O.; Kotov, N. A. *Angew. Chem., Int. Ed.* **2005**, *44*, 7439−7442. (i) Wang, S.; Westcott, S.; Chen, W. *J. Phys. Chem. B* **2002**, *106*, 11203−11209.

(8) (a) Fischer, L. H.; Harms, G. S.; Wolfbeis, O. S. *Angew. Chem., Int. Ed.* **2011**, *50*, 4546−4551. (b) Vetrone, F.; Naccache, R.; Zamarrn, A.; de la Fuente, A. J.; Sanz-Rodrguez, F.; Maestro, L. M.; Rodriguez, E. M.; Jaque, D.; Sol, J. G; Capobianco, J. A. *ACS Nano* **2010**, *4*, 3254−3258. (c) Borisov, S. M.; Gatterer, K.; Bitschnau, B.; Klimant, I. *J. Phys. Chem. C* **2010**, *114*, 9118−9124. (d) Borisov, S. M.; Wolfbeis, O. S. *Anal. Chem.* **2006**, *78*, 5094−5101. (e) Dos Santos, P. V.; De Araujo, M. T.; Gouveia-Neto, A. S.; Medeiros Neto, J. A.; Sombra, A. S. B. *IEEE J. Quantum Electron.* **1999**, *35*, 395−399. (f) Samulski, T. V.; Chopping, P. T.; Haas, B. *Phys. Med. Biol.* **1982**, *27*, 107−114.

(9) (a) Carbone, L.; Nobile, C.; De Giorgi, M.; Della Sala, F.; Morello, G.; Pompa, P.; Hytch, M.; Snoeck, E.; Fiore, A.; Franchini, I. R.; Nadasan, M.; Silvestre, A. F.; Chiodo, L.; Kudera, S.; Cingolani, R.; Krahne, R.; Manna, L. *Nano Lett.* **2007**, *7*, 2942−2950. (b) Talapin, D. V.; Koeppe, R.; Götzinger, S.; Kornowski, A.; Lupton, J. M.; Rogach, A. L.; Benson, O.; Feldmann, J.; Weller, H. *Nano Lett.* **2003**, *3*, 1677−1681.

(10) (a) Mishra, A.; Behera, R. K.; Behera, P. K.; Mishra, B. K.; Behera, G. B. *Chem. Rev.* **2000**, *100*, 1973−2011. (b) Widengren, J.; Schwille, P. *J. Phys. Chem. A* **2000**, *104*, 6416−6428. (c) Heilemann, M.; Margeat, E.; Kasper, R.; Sauer, M.; Tinnefeld, P. *J. Am. Chem. Soc.* **2005**, *127*, 3801−3806. (d) Weston, K. D.; Carson, P. J.; Metiu, H.; Buratto, S. K. *J. Chem. Phys.* **1998**, *109*, 7474−7485. (e) Soper, S. A.; Mattingly, Q. L. *J. Am. Chem. Soc.* **1994**, *116*, 3744−52.

(11) (a) Chan, E. M.; Xu, C.; Mao, A. W.; Han, G.; Owen, J. S.; Cohen, B. E.; Milliron, D. J. *Nano Lett.* **2010**, *10*, 1874−1885. (b) Rosen, E. L.; Buonsanti, R.; Llordes, A.; Sawvel, A. M.; Milliron, D. J.; Helms, B. A. *Angew. Chem., Int. Ed.* **2012**, *51*, 684−689.

(12) (a) Varshni, Y. P. *Physica* **1967**, *34*, 149−154. (b) Valerini, D.; Cretí, A.; Lomascolo, M. *Phys. Rev. B* **2005**, *71*, 235409.

(13) Bayles, A. R.; Chahal, H. S.; Chahal, D. S.; Goldbeck, C. P.; Cohen, B. E.; Helms, B. A. *Nano Lett.* **2010**, *10*, 4086−4092.

(14) (a) Lees, E. E.; Gunzburg, M. J.; Nguyen, T. L.; Howlett, G. J.; Rothacker, J.; Nice, E. C.; Clayton, A. H.; Mulvaney, P. *Nano Lett.* **2008**, *8*, 2883−2890. (b) Cedervall, T.; Lynch, I.; Lindman, S.; Berggård, T.; Thulin, E.; Nilsson, H.; Dawson, K. A.; Linse, S. *Proc. Natl. Acad. Sci. U.S.A.* **2007**, *104*, 2050−2055. (c) Röcker, C.; Pötzl, M.; Zhang, F.; Parak, W. J.; Nienhaus, G. U. *Nat. Nanotechnol.* **2009**, *4*, 577−580.

(15) (a) Berlier, J. E.; Rothe, A.; Buller, G.; Bradford, J.; Gray, D. R.; Filanoski, B. J.; Telford, W. G.; Yue, S.; Liu, J.; Cheung, C.-Y.; Chang, W.; Hirsch, J. D.; Beechem, J. M.; Haugland, R. P.; Haugland, R. P. *J. Histochem. Cytochem.* **2003**, *51*, 1699−1712. (b) Luby-Phelps, K.; Mujumdar, S.; Mujumdar, R. B.; Ernst, L. A.; Galbraith, W.; Waggoner, A. S. *Biophys. J.* **1993**, *63*, 236−242.